Available online at www.sciencedirect.com
SCIENCE DIRECT®
International Journal of Thermal Sciences 43 (2004) 277–287
International Journal of Thermal Sciences
www.elsevier.com/locate/ijts

Numerical and experimental investigation of melting and freezing processes in phase change material storage

Piia Lamberg [a], Reijo Lehtiniemi [b,*], Anna-Maria Henell [b]

[a] *Helsinki University of Technology, Laboratory of Heating, Ventilating and Air-Conditioning, P.O. Box 4400, 02015 HUT, Finland*
[b] *Nokia Research Center, P.O. Box 407, 00045 Nokia Group, Finland*

Received 4 March 2003; accepted 2 July 2003

Abstract

Phase change material (PCM) storages are used to balance temporary temperature alternations and to store energy in several practical application areas, from electronics to the automobile industry and also buildings. In current telecommunication electronics both portable and larger scale thermal transients that occur due to temporarily varying power dissipation are customary. The use of PCM heat storage to compensate for temperature peaks that may occur offer significant savings in time-dependent thermal management in the aforementioned products.

The aim of this paper was to obtain physical validation of the numerical results produced using FEMLAB. This validation was obtained through a comparison of experimental data and numerical results. The numerical methods studied were an enthalpy method and an effective heat capacity method. An ensemble of experimental PCM storages, with and without heat transfer enhancement structures, was designed and constructed. The numerical predictions calculated with FEMLAB simulation software were compared to experimental data. Both numerical methods gave good estimations for the temperature distribution of the storages in both the melting and freezing processes. However, the effective heat capacity method, which used a narrower temperature range, $dT = 2\,^{\circ}C$, was the most precise numerical method when the numerical results were compared to the experimental results.

Keywords: Phase change materials; Effective heat capacity method; Enthalpy method

1. Introduction

Phase change material (PCM) storages are used to balance temporary temperature alternations and to store energy in several practical application areas, from electronics to the automobile industry and also in buildings. PCM storage is preferable to sensible heat storage in applications with a small temperature swing because of its nearly isothermal storing mechanism and high storage density. When a temperature peak occurs, PCM absorbs the excessive energy by going through a phase transition and releasing the absorbed energy later when the peak has passed off. The storage can be dimensioned in such a way that the temperature of the storage is kept under a specified temperature level whilst at the same time the excess external energy is stored.

In current telecommunication electronics, both portable and larger scale thermal transients that occur due to temporarily varying power dissipation are customary. The use of PCM heat storage to compensate for temperature peaks that may occur offer a significant savings in the time-dependent thermal management of the aforementioned products, providing that the thermal behaviour of the system is known. In addition, the system has to be optimised in line with allowed temperatures, heat loads, their durations and locations, weight, dimensions and other mechanical restrictions.

Since the conditions to be optimised may vary significantly and change rapidly in the course of the design process, a straightforward, reliable PCM model would enable parametric studies to be conducted at speed and would also enable the comparison of several alternatives without having to build large, time-consuming full-scale FEM models. This would also preclude the need to build experimental platforms for measurements.

Heat transfer in PCM storage is a transient, non-linear phenomenon with a moving solid–liquid interface, gener-

* Corresponding author.
E-mail addresses: piia.lamberg@hut.fi (P. Lamberg), reijo.lehtiniemi@nokia.com (R. Lehtiniemi).

1290-0729/$ – see front matter
doi:10.1016/j.ijthermalsci.2003.07.001

Nomenclature

D	height of the storage	m
g	acceleration of gravity	$m{\cdot}s^{-2}$
c_p	specific heat	$J{\cdot}kg^{-1}{\cdot}K^{-1}$
k	heat conductivity	$W{\cdot}m^{-1}{\cdot}K^{-1}$
h_c	convection heat transfer coefficient	$W{\cdot}m^{-2}{\cdot}K^{-1}$
H	enthalpy	J
l	length of the storage	m
L	latent heat of fusion	$J{\cdot}kg^{-1}$
$\underline{n}$	outward unit normal	
p	pressure	Pa
S	the location of the solid–liquid interface in y-direction	m
t	time	s
T	temperature	°C
u	solution	
$\bar{v}$	velocity	$m{\cdot}s^{-1}$
x, y, z	dimensions and directions	

PDE coefficient

$d_a, F, G, R, \Gamma, c, \alpha, \gamma, g, q, h$ and r

Greek symbols

α	thermal diffusivity	$m^2{\cdot}s^{-1}$
β	coefficient of the thermal expansion	$°C^{-1}$
λ	Lagrange multiplier	
μ	dynamic viscosity	$kg{\cdot}m^{-1}{\cdot}s^{-1}$
ρ	density	$kg{\cdot}m^{-3}$
Ω	domain	
$\partial\Omega$	boundary of the domain	

Subscripts

eff	effective
c	convection
i	initial
l	liquid
m	melting
n	normal
o	reference conditions
p	phase change
s	solid
w	wall

ally referred to as the "moving boundary" problem. Nonlinearity is the source of difficulties in moving boundary problems [1,2] and, therefore, analytical solutions for phase change problems are only known for a couple of physical situations that have a simple geometry and simple boundary conditions. The most well-known precise analytical solution for a one-dimensional moving boundary problem, called the Stefan problem, was originated by Neumann [1,3]. Some analytical approximations for one-dimensional moving boundary problems with different boundary conditions have been produced. These include the quasi-stationary approximation, perturbation methods, the Megerlin method and the Heat-balance-integral method [1]. In these methods, it has been assumed that the melting or solidification temperature is constant. However, technical grade paraffin, for example, has a wide temperature range at the points where melting and solidification occur. Also, the aforementioned methods are only suitable for calculating semi-infinite or infinite storage, however in reality storages are finite and have to be handled three- or at least two-dimensionally so as to achieve a sufficiently accurate solution. Therefore, numerical methods have to be used to achieve a sufficiently accurate solution for heat transfer in PCM storage.

Phase change problems are usually solved with finite difference or finite element methods in accordance with the numerical approach. The phase change phenomenon has to be modelled separately due the non-linear nature of the problem. A wide range of different kinds of numerical methods for solving PCM problems exist. The most common methods used are the enthalpy method and the effective heat capacity method. These methods are able to use PCMs with a wide phase change temperature range. The enthalpy method is introduced in many references as a numerical method for solving phase change problems [1,3,4]. The method is based on the weak solution of partial different equations.

Voller et al. have presented a simple development of the conventional enthalpy formulation which leads to very accurate solutions. The extension of this technique to two-dimensional problems is demonstrated by using an explicit method. A relative accuracy of 0.1% has been obtained in the comparison between numerical results achieved by other authors and the results achieved with the developed method [5].

Costa et al. have used the enthalpy formulation with a fully implicit finite difference method to analyse numerically the thermal performance of latent heat storage. The method takes into account both conduction and convection heat transfer in a one-dimensional model and conduction in a two-dimensional model. The method used was validated by comparing the results with other analytical and numerical results found from the literature. The conclusion is that the method is useful for designing a thermal energy storage [6].

In the effective heat capacity method the latent heat effect is expressed as a finite temperature dependent specific heat which occurs over a temperature range.

Bonacina et al. have presented the one-dimensional three-time level difference method in which the latent heat effect is defined by a large heat capacity over a small temperature range. The phase change was assumed to take place in a temperature range interval of 0.5 °C. The numerical results obtained are satisfactory when compared with the available analytical solutions. The conclusion of the paper is that an

accuracy of 3% for the numerical results when compared to the analytical results is well within the limits imposed for engineering calculations [7].

The multidimensional numerical solution based on a large heat capacity over the phase change temperature range is presented by Rabin et al. [8]. The phase change problem is solved using the finite difference method. The computation technique is able to consider all kinds of boundary conditions, i.e., conduction, convection and radiation, either alone or in combination. The proposed method is verified against two exact solutions and against two numerical solutions available from the literature. The comparison showed a good agreement with different boundary conditions [8].

The aim of this paper was to obtain a physical validation of the numerical results produced using FEMLAB [9]. This validation was obtained through a comparison of experimental data and numerical results. Two experimental PCM storages, with and without heat transfer enhancement structures, were designed and constructed. The numerical results calculated with two different kinds of numerical methods were compared with the experiment results achieved by using thermocouples mounted inside the storage.

Usually the computational models for a two- or three-dimensional PCM storage are complicated to develop and modelling different kinds of geometry or dimensions may cause problems. The use of the FEMLAB programme would save time and energy in routine engineering work.

2. Theory

The melting and solidification processes in two different kinds of PCM storage is studied numerically and experimentally (see Figs. 1 and 2). In storage 1, there is no heat transfer enhancement structure but in storage 2 there are two fins inside the storage. The storages are filled with PCM. Two side walls are imposed onto the temperature change. The two remaining walls are insulated.

In the melting process, heat transfers from the walls to the phase change material first by conduction and later by natural convection. Natural convection speeds up the melting process. With Rayleigh's number it is possible to determine when the dominant heat transfer mode turns from conduction to convection. When $Ra \geqslant 10^3$, the liquid PCM starts to flow up along the vertical hot wall surface and then falls down along the cold solid–liquid interface causing natural convection [10]. The effect of natural convection in the molten PCM causes a higher rate of melting near the top of the enclosure. In the early stage of melting, the velocity of the liquid PCM due to the buoyancy force is small. It increases and convection in the melt becomes dominant until the magnitude of the velocity begins to decrease due to the temperature difference in the liquid PCM becoming more uniform [11].

The main heat transfer mode is conduction during the solidification process. Natural convection exists in the liquid–solid interface due to the temperature difference in the liquid PCM. But even a very strong natural convection in the solid–liquid interface has a negligible effect on the solid–liquid interface position compared to the effect of heat conduction in solid PCM [12].

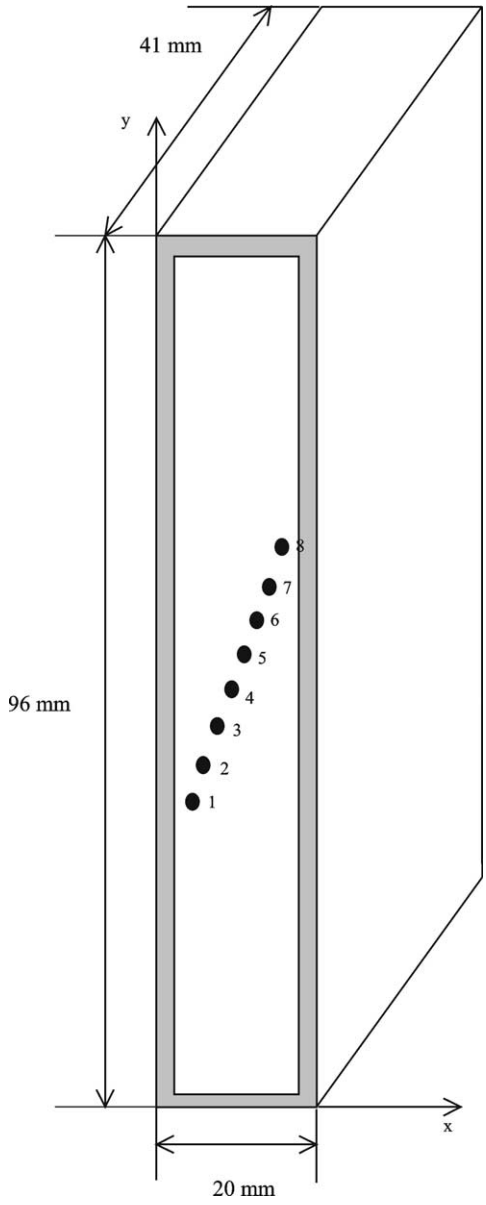

Storage 1 Thermocouple	*x* [mm]	*y* [mm]
1	1.191	25.4
2	3.92	31.02
3	6.38	36.16
4	8.73	42.17
5	11.28	47.3
6	13.47	53.13
7	15.62	58.99
8	17.26	64.32

Fig. 1. Storage 1. The storage without fins.

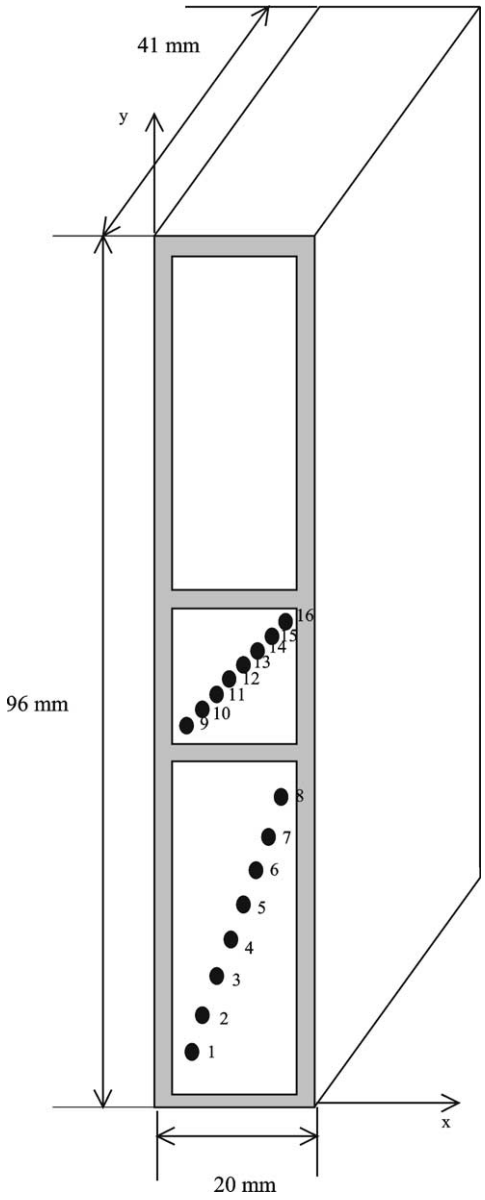

Storage 2 Thermocouple	*x* [mm]	*y* [mm]
1	2.238	8.123
2	4.598	11.185
3	6.382	14.16
4	8.577	18.16
5	11.312	21.261
6	13.663	23.961
7	15.579	27.75
8	17.12	31.844
9	1.956	40.238
10	4.599	41.731
11	6.536	44.198
12	8.565	46.391
13	9.693	48.342
14	12.078	51.444
15	14.629	53.647
16	16.531	55.821

Fig. 2. Storage 2. The storage with fins.

The governing equations for transient analyses of the melting of the phase change material includes the Navier–Stokes (momentum) equations, the continuity equation, and the energy equation. The Boussinesq approximation is used to model the buoyancy forces. The equations are the following, given in tensor notation [13,14]:

$$\rho\frac{\partial\vec{v}}{\partial t}+\rho\big(\vec{v}\cdot\nabla\big)\vec{v}=-\nabla p+\mu\nabla^2\vec{v}+\rho\vec{g}\beta(T-T_o) \tag{1}$$

$$\nabla\cdot\vec{v}=0 \tag{2}$$

$$\rho_l c_{pl}\left(\frac{\partial T_1}{\partial t}+\vec{v}\cdot\nabla T_l\right)=\nabla(k_l\nabla T_l) \tag{3}$$

where ρ_l is the density, $\bar{v}$ the velocity of the liquid PCM, p the pressure, μ the dynamic viscosity, $\vec{g}$ the gravity vector, β the coefficient of thermal expansion, T_o the reference temperature, c_l the specific heat, k_l the heat conductivity and T_l the temperature of the liquid PCM.

For the solid PCM and the enclosure the Eqs. (1), (2) can be ignored because there is no convection effect on the materials. The energy equation is given the form

$$\rho_s c_{ps}\left(\frac{\partial T_s}{\partial t}\right)=\nabla(K_s\nabla T_s) \tag{4}$$

where subscript s denotes the solid PCM or the enclosure.

The energy balance for the solid–liquid interface in the melting process is given the form [3]:

$$k_s\frac{\partial T_s}{\partial\underline{n}}\Big|_s-k_l\frac{\partial T_s}{\partial\underline{n}}\Big|_s=\rho_s L\frac{\mathrm{d}S_n}{\mathrm{d}t} \tag{5}$$

where S is the solid–liquid phase change interface, $\underline{n}$ the normal of the solid–liquid interface and L the latent heat of the PCM fusion. In the solidification process the subscripts l and s are interchanged and the latent heat of fusion L is replaced with $-L$ in Eq. (5).

The temperatures of the solid and the liquid PCM are equal in the solid–liquid interface.

$$T_l=T_s \tag{6}$$

3. Experimental configuration and procedure

3.1. Phase change material used in the experiments

The phase change material used in the experiments is technical grade paraffin. The material is both an ecologically and environmentally friendly material that utilises processes between the solid and liquid phase change to store and release energy within the small temperature range. The volume change is minor between the solid and liquid phase and it is also 100% recyclable. The material properties of the PCM are presented in Table 1.

To find out the behaviour of the PCM during the melting and freezing process the DSC measurements are performed with Mettler TA4000 thermoanalysis equipment with a liquid nitrogen cooling system. The measurement is performed

with a heating and cooling speed of 2 °C·min^{-1}. The DSC-curve for the melting and freezing processes of the paraffin is shown in Fig. 3.

The material starts melting when it achieves a temperature of 20–21 °C. The peak temperature of the melting is 27.7 °C. At the peak temperature the material stores or releases the greatest amount of energy. Solidification starts when the material achieves a temperature of 26.5 °C and the peak temperature of the solidification is 23 °C. The latent heat energy is released completely when the temperature of the material approaches 21 °C.

Table 1
The material properties of technical grade paraffin

	Paraffin
Density solid/liquid 15/70 °C (ρ) kg·m^{-3}	789/750
Heat conductivity solid/liquid (k) W·m^{-1}·K^{-1}	0.18/0.19
Heat capacity solid/liquid (c_p) KJ·kg^{-1}·K^{-1}	1.8/2.4
Volume expansion at $\Delta T = 20$ °C, %	4.9
Heat storage capacity melting $\Delta T = 30$ °C, J·kg^{-1}	175 066
Heat storage capacity solidification $\Delta T = 30$ °C, J·kg^{-1}	187 698

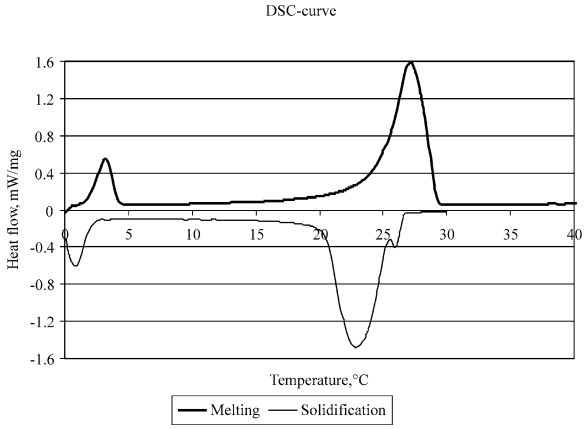

Fig. 3. The DSC-curve of the paraffin.

3.2. Experimental set-up

In order to provide a well-controlled environment for the evaluation of the simulation results, two specific PCM storages were manufactured: one simple container (Fig. 1), and one equipped with internal fins to enhance heat transfer from the walls to the PCM (Fig. 2).

The heat storages for the measurements were fabricated from solid Aluminium (AlSi1MgT6, $k = 174$ W·m^{-1}·K^{-1}) blocks by machining the interior off using the electro-discharge method to ensure flawless heat transfer in the aluminium without any additional contact resistances due to joints.

The storages were equipped with Watlow Gordon K-type thermocouples of 40 AWG (approximately 0.08 mm) diameter that were arranged as shown in Figs. 1 and 2. The measurement points were set at about 2 mm intervals in the direction of the heat transfer on special comb-like supports.

The supports were fabricated from a 300 μm thick FR4 epoxy-glass fibre composite, the heat conductivity of which is as low as 0.3 W·m^{-1}·K^{-1}. Due to their thinness and low conductivity, the effect of the supports on the PCM behaviour was neglected. The as-thin-as convenient thermocouple wires were guided out of the storage in the

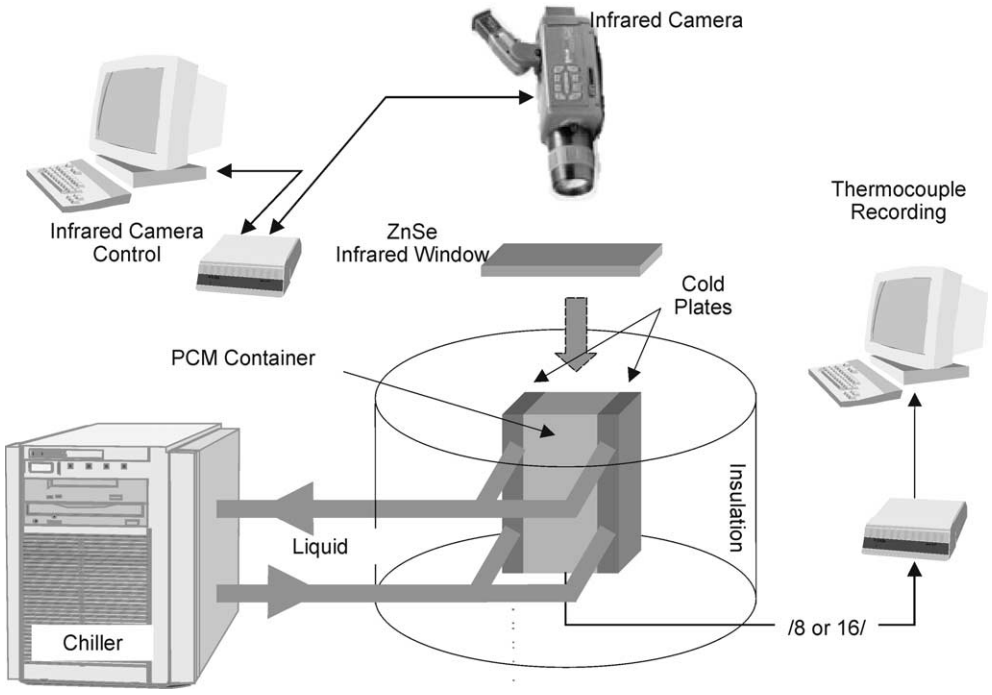

Fig. 4. The measurement set-up.

direction of the isotherms to minimise their disturbance to the system.

The bottom of the container was sealed with chemically inert nitrile rubber mounted between the container and the bottom block to prevent leakage. The bottom block was made of a Tufnol phenolic fabric with a low through-plane thermal conductivity of 0.37 $W \cdot m^{-1} \cdot K^{-1}$. The measurement set-up is schematically shown in Fig. 4.

After mounting and filling the storages to halfway with technical grade paraffin, the positions of the thermocouple sensors were determined optically with 0.01 mm accuracy and the filling was continued. Due to a volume expansion of about 5%, the corresponding container space at the top of the container was left empty after PCM solidification.

Two identical Aavid 6063-T5 Aluminium cold plates with an optimal coolant current of 4 $l \cdot min^{-1}$ were mounted on opposite sides of the container to provide symmetry in the direction of the heat transfer. The cold plates and the remaining walls of the storage were isolated from the room temperature environment with Styrofoam. The coolant liquid was water, the temperature and circulation of which was controlled by a Lauda RM6 liquid circulation chiller, which produces a preset temperature liquid flow (nominally 0.15 $l \cdot s^{-1}$) and keeps the liquid temperature steady at 0.1 °C accuracy by employing its own thermostatically controlled cooler and heater, or alternatively, it measures the temperature of the liquid used in circulation.

3.3. Measurements

In the measurements, the liquid circulation chiller was first set to cool the cold plates to +10 °C. When a steady state was reached, the cooling water temperature was set to +40 °C and the system was allowed to develop towards the new equilibrium. The up ramp stage for the cold plates typically took about 15 minutes. After all the PCM had melted and the system was in a +40 °C steady state, the cooling water temperature was then set to +10 °C. The cooling phase of the cycle typically lasted about 80 minutes.

The entire 10 °C–40 °C–10 °C cycle took about 2.5–3 hours and it was repeated at least five times for each measurement case. For each cycle, the temperature responses were for either eight (storage 1) or 16 (storage 2) thermocouples (see Figs. 1 and 2).

4. Numerical methods

4.1. Enthalpy method

In reality in phase change situations more than one phase change interface may occur or the interfaces may disappear entirely. Furthermore, the phase change usually happens in a non-isothermal temperature range, such as in the case of paraffin. In such cases tracking the solid–liquid interface may be difficult or even impossible. From the point of view of the calculation it is advantageous that the problem is reformulated in such a way that the Stefan condition is implicitly bound up in a new form of the equations and that the equations are applied over the whole fixed domain. This can be done by determining what is known as the enthalpy function $H(T)$ for the material. This determines the sum of the sensible heat and the latent heat required for the phase change [4].

In this paper the natural convection effect is simulated through a heat transfer coefficient. The term $(\rho c_p \vec{v} \cdot \nabla T_l)$ is replaced with the term $(h_c \nabla T)$ in Eq. (3), and Eqs. (1) and (2) are ignored. The enthalpy form for energy equation (Eq. (3)) with initial and boundary conditions is given the form

$$\rho \frac{\partial H}{\partial t} + h_c \nabla T = \nabla (k \nabla T) \tag{7}$$

$$T(x, y, z, 0) = T_i \tag{8}$$

$$T(0, y, z, t) = T(l_x, y, z, t) = T_w(t) \tag{9}$$

$$\frac{\partial T(x, 0, z, t)}{\partial y} = \frac{\partial T(x, l_y, z, t)}{\partial y} = 0 \tag{10}$$

$$\frac{\partial T(x, y, 0, t)}{\partial z} = \frac{\partial T(x, y, l_z, t)}{\partial z} = 0 \tag{11}$$

where H is the enthalpy, l is the length of the storage. The subscript i denotes initial, w the wall, x the x-direction, y the y-direction and z the z-direction.

Lamberg et al. [15] have performed this equation to establish the convection heat transfer coefficient in a rectangular store containing paraffin in accordance with studies by Marshall [16,17] and Eftekhar et al. [18]. The convection heat transfer coefficient during the melting process is

$$h_c = 0.072 \left[\frac{[g((T_w - T_m)/2)\rho_l^2 c_{pl} k_l^2 \beta]}{\mu} \right]^{1/3} \tag{12}$$

The great advantage of the enthalpy method is that it can be used with any material and not just with phase change materials. For the phase change material it is possible to determine the enthalpy function $H(T)$ by considering the results of the DSC-measurements.

4.2. Effective heat capacity method

With effective heat capacity it is also possible to describe the non-isothermal phase change in the PCM. The effective heat capacity of the material (c_{eff}) is directly proportional to the stored and released energy during the phase change and the specific heat. However, it is inversely proportional to the width of the melting or solidification temperature range [19]. During the phase change the effective heat capacity of the PCM is

$$c_{\text{eff}} = \frac{L}{(T_2 - T_1)} + c_p \tag{13}$$

where T_1 is the temperature where melting or solidification begins and T_2 the temperature where the material is totally

Table 2
The coefficient terms

The method	d_a	Γ	F
Enthalpy method	$\rho\frac{\partial H(T)}{\partial t} = \rho c_p(T)\frac{\partial T}{\partial t}$	$\Gamma = k\left(\frac{\partial T}{\partial x} + \frac{\partial T}{\partial y}\right)$	$F = h_c\left(\frac{\partial T}{\partial x} + \frac{\partial T}{\partial y}\right)$
Effective heat capacity method	$\rho c_p\frac{\partial T}{\partial t}$	$\Gamma = k\left(\frac{\partial T}{\partial x} + \frac{\partial T}{\partial y}\right)$	$F = h_c\left(\frac{\partial T}{\partial x} + \frac{\partial T}{\partial y}\right)$

melted or solidified. The effective heat capacity of the paraffin can be defined separately for the melting and freezing processes by using DSC-measurements.

The energy equation (Eq. (3)) with initial and boundary conditions is

$$\rho_l c_p\frac{\partial T_1}{\partial t} + h_c\nabla T = \nabla(k_l\nabla T_1) \tag{14}$$

$$T(x, y, z, 0) = T_i \tag{15}$$

$$T(0, y, z, t) = T(l_x, y, z, t) = T_w(t) \tag{16}$$

$$\frac{\partial T(x, 0, z, t)}{\partial y} = \frac{\partial T(x, l_y, z, t)}{\partial y} = 0 \tag{17}$$

$$\frac{\partial T(x, y, 0, t)}{\partial z} = \frac{\partial T(x, y, l_z, t)}{\partial z} = 0 \tag{18}$$

where

$$c_p = \begin{cases} c_{ps}, & T < T_1 \\ \frac{L}{(T_2 - T_1)} + c_p, & T_1 \leqslant T \leqslant T_2 \\ c_{pl}, & T > T_2 \end{cases} \tag{19}$$

4.3. Numerical calculations with FEMLAB

The calculations are done for the same melting and solidification cycles as would be the case in experiments, and the temperature of the wall sand the boundary conditions Eqs. (7)–(12) are defined in accordance with these experiments.

In numerical calculations several assumptions are made. It has been assumed that the heat conductivity and density of the phase change material and the enclosure are constant. The values for the PCM are chosen as average values of the solid and liquid material properties, ($k_p = 0.185$ W·m^{-1}·K^{-1} and $\rho_p = 770$ kg·m^{-3}). The problem is handled two-dimensionally. The heat transfer in the z-direction is assumed to be negligible. It is also assumed that the convection heat transfer coefficient in the liquid PCM during the solidification process is negligible.

The numerical calculation is performed with FEMLAB software. This is designed to simulate systems of coupled non-linear and time dependent partial differential equations (PDE) in one-, two- or three-dimensions. The programme can be used to simulate any system of coupled PDEs in the areas of heat transfer, electromagnetism, structural mechanics and fluid dynamics. The FEMLAB software operates in the MatLab environment [20].

The geometry of the storage is defined. The equations for the metal housing and the PCM are written in partial differential form in line with programme definitions, and initial and boundary conditions are determined.

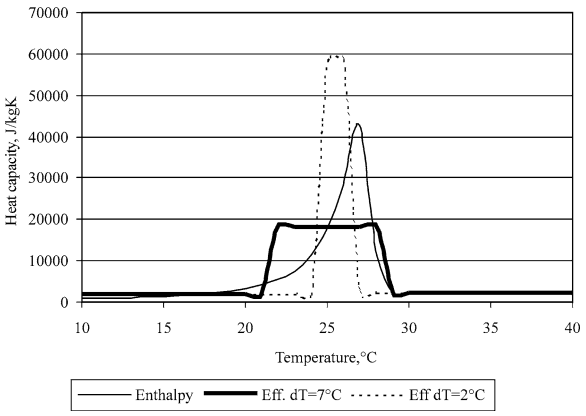

Fig. 5. The specific heat capacities in the melting process in enthalpy and heat capacity methods. Enthalpy denotes the enthalpy method, Eff d$T = 7\,^\circ$C the effective heat capacity method with a large temperature range and Eff d$T = 2\,^\circ$C the effective heat capacity method with a narrow temperature range.

The general form of the PDEs and boundary conditions is defined as

$$d_a\frac{\partial u}{\partial t} + \nabla\cdot\Gamma = F \quad \text{in } \Omega \tag{20}$$

$$\underline{n}(c\nabla u + \alpha u - \gamma) + qu = g - \lambda \quad \text{on } \partial\Omega \tag{21}$$

$$hu = r \quad \text{on } \partial\Omega \tag{22}$$

where u is the solution and Γ and F coefficient terms which can be functions of the space, time, the solution u or its gradient. Ω is the observed domain, $\partial\Omega$ the boundary of the domain, n the outward unit normal, λ an unknown vector-valued function called the Lagrance multiplier. This multiplier is only calculated in scenarios where mixed boundary conditions exist. The coefficients d_a, c, α, γ, g, q, h and r are scalars, vectors, matrices or tensors. Their components can be functions of space, time, and the solution u.

In Table 2 the coefficient terms of the general form (Eq. (20)) of the enthalpy method and the effective heat capacity method are presented. In the boundaries which are insulated, the coefficient terms α, γ, g, q, λ, h and r are given the value zero in both methods. The two side walls which are heated or cooled according to the coefficient terms c, α, γ, g, q and λ are given the values zero. h is given values 1 and r value $T_w(t)$.

In the melting process when the PCM is solid ($T_p < T_1$) and during the solidification process the term F is given the value zero ($F = 0$) because the convective heat transfer is only taken into account in the melting process when the PCM is in a liquid state. The numerical calculations are performed using an enthalpy method and with the effective

Table 3
The specific heat and convective heat transfer coefficient of the paraffin in numerical calculations

Paraffin $c_p(T)$	Melting	Solidification
Enthalpy method	$c_p(T) = \begin{cases} 24T^2 + 515T + 3606, & 10\,^\circ\mathrm{C} \leqslant T < 20\,^\circ\mathrm{C} \\ 146T^3 - 9123T + 191\,658, & 20\,^\circ\mathrm{C} \leqslant T \leqslant 27\,^\circ\mathrm{C} \\ 11\,285T^2 - 652T + 9424, & 27\,^\circ\mathrm{C} \leqslant T \leqslant 29\,^\circ\mathrm{C} \\ 2400, & T > 29\,^\circ\mathrm{C} \end{cases}$	$c_p(T) = \begin{cases} 32T^2 - 671T + 4548, & 10\,^\circ\mathrm{C} \leqslant T < 19\,^\circ\mathrm{C} \\ 3205T^2 - 124\,276T + 1\,207\,500, & 19\,^\circ\mathrm{C} \leqslant T \leqslant 23\,^\circ\mathrm{C} \\ -11\,543T^2 + 536\,878T - 6\,197\,600, & 23\,^\circ\mathrm{C} < T \leqslant 25\,^\circ\mathrm{C} \\ -7374T + 194\,125, & 25\,^\circ\mathrm{C} < T \leqslant 26\,^\circ\mathrm{C} \\ 2400, & T > 26\,^\circ\mathrm{C} \end{cases}$
	$h_c = 75\ \mathrm{W{\cdot}m^{-2}{\cdot}K^{-1}}$ when $T > 20\,^\circ\mathrm{C}$	$h_c = 0\ \mathrm{W{\cdot}m^{-2}{\cdot}K^{-1}}$
Effective heat capacity method	$c_p(T) = \begin{cases} 1800, & T < 21 \\ 18\,067, & 21 \leqslant T \leqslant 28 \\ 2400, & T > 28 \end{cases}$	$c_p(T) = \begin{cases} 1800, & T < 20 \\ 26\,740, & 20 \leqslant T \leqslant 25 \\ 2400, & T > 25 \end{cases}$
	$h_c = 75.03\ \mathrm{W{\cdot}m^{-2}{\cdot}K^{-1}}$ when $T > 21\,^\circ\mathrm{C}$	$c_p(T) \begin{cases} 1800, & T < 25 \\ 127\,698, & 25 \leqslant T \leqslant 27 \\ 2400, & T > 27 \end{cases}$
	$c_p(T) \begin{cases} 1800, & T < 25 \\ 116\,866, & 25 \leqslant T \leqslant 27 \\ 2400, & T > 27 \end{cases}$	$h_c = 0\ \mathrm{W{\cdot}m^{-2}{\cdot}K^{-1}}$
	$h_c = 69\ \mathrm{W{\cdot}m^{-2}{\cdot}K^{-1}}$ when $T > 25\,^\circ\mathrm{C}$	

heat capacity method with two different temperature ranges ($T_2 - T_1$). The temperature ranges are

- narrow temperature range, melting $\mathrm{d}T = T_2 - T_1 = 27$–$25\,^\circ\mathrm{C}$, solidification $\mathrm{d}T = T_2 - T_1 = 25$–$27\,^\circ\mathrm{C}$ and
- wide temperature range, melting $\mathrm{d}T = T_2 - T_1 = 28$–$21\,^\circ\mathrm{C}$, solidification $T_2 - T_1 = 20$–$25\,^\circ\mathrm{C}$.

Table 3 presents the specific heat capacities and the convective heat transfer coefficients for the paraffin used in the numerical calculations in the temperature range of 10–40 °C in both the melting and freezing processes. In these calculations the specific heat is assumed to be continuous.

Fig. 5 presents the specific heat in the function of the temperature in different numerical methods in the melting process.

The total storage capacity of the PCM in the temperature range 10–40 °C is the same in all the given methods.

5. Comparison between numerical model predictions and experimental data

5.1. Storage 1. The storage without fins

The temperature of the PCM is calculated numerically at eight measurement points in the storage without the fins. The points are presented in Figs. 1 and 2. The numerical and experimental results of the temperature of the PCM at points 2, 4, 5 and 7 and the wall temperature of the coldplates are presented in Fig. 6. Exp denotes experimental results, Ent the numerical results calculated using the enthalpy method, Eff_2 the numerical results calculated using the effective method with a narrow temperature range ($\mathrm{d}T = 2\,^\circ\mathrm{C}$) and Eff_7 the numerical results calculated using an effective method with a wide temperature range ($\mathrm{d}T = 7\,^\circ\mathrm{C}$).

During the melting process all the numerical methods give almost the same results for the temperature of the PCM when the PCM is in a solid state. First of all the PCM starts to melt when the effective heat capacity method with a wide temperature range is used. The melting starts at 20 °C. However, quite soon after the effect of natural convection uniforms the temperature development of the PCM in all the numerical methods. The PCM melts a little too quickly at points 2 and 7 when the experimental and numerical results are compared. All the numerical results compare quite well to the experimental results of the temperature of the PCM.

The effect of the natural convection in the liquid PCM seems to be modelled quite well in the numerical methods despite the value of the convective heat transfer coefficient being estimated according to the melting temperature and the maximum coldplate temperature during the process.

During the solidification process all the numerical methods give uniform results for the temperature of the PCM in a liquid state. When solidification begins the effective heat capacity method with a wide temperature range gives almost the same results as the enthalpy method but differs from the results achieved with the effective heat capacity method with a narrow phase change range. However, the effective heat capacity method with a narrow temperature range best follows the experimental results when the phase change occurs.

The error when the numerical and experimental results are compared is small. The most precise numerical method is the effective heat capacity method with a narrow temperature

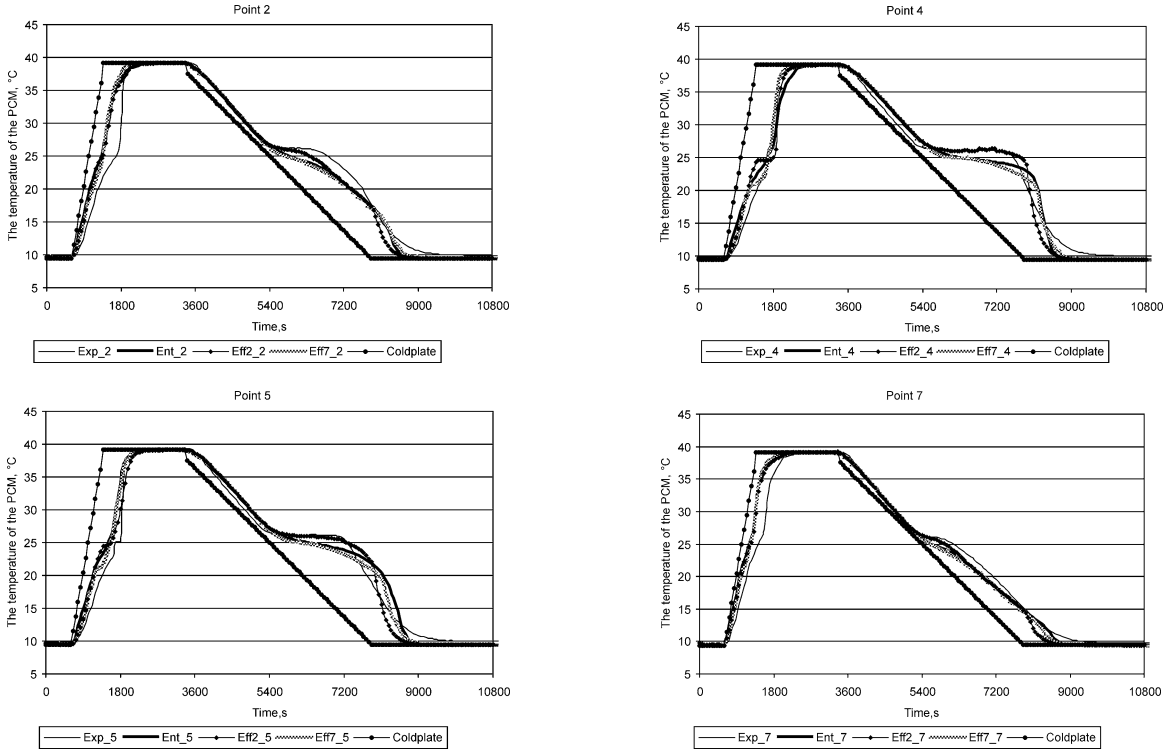

Fig. 6. The temperature of the PCM at measurement points 2, 4, 5 and 7 in the PCM storage without internal fins, storage 1.

range for the technical grade paraffin used in these experiments in storage 1.

5.2. Storage 2. The PCM storage with two fins

Fig. 7 shows the temperature of the PCM at points 2, 4, 6, 10, 12 and 14 in the PCM storage with two fins. Exp denotes the experimental results, Ent the numerical results calculated with the enthalpy method, Eff_2 the numerical results calculated with the effective method ($dT = 2\,^{\circ}C$) and Eff_7 the numerical results calculated with the effective method ($dT = 7\,^{\circ}C$).

The phenomena which were observed in the storage without fins can also been seen in the results from the storage with the fins. During the melting process the numerical methods give the most precise results for the temperature of the PCM in the middle of the storage at points 4 and 12. At the sides of the storage the PCM melts too quickly.

In the solidification process the numerical results for the temperature of the PCM follow the experimental results well when the PCM is in a liquid state. The effective heat capacity method with a narrow temperature range gives the most precise result for the temperature of the PCM compared to the numerical results.

In conclusion, all the numerical results give a good estimation of the melting and freezing processes while the effective heat capacity method with a narrow temperature range, $dT = 2\,^{\circ}C$, is the most precise method.

6. Discussion

When numerical methods are used, it seems that the biggest error is made when the material is solid. The most evident reason for the difference between the numerical and experimental results may be in the thermal contact resistance between the coldplate and the PCM container. Thermal contact resistance was not taken into account in the simulations. It was assumed that the walls of the PCM container are at the same temperature as the circulated liquid. The absence of thermal contact resistance may explain the deviations between the simulations and experiment results in the solid state.

One reason for the difference between the numerical and experimental results is in the material properties of the PCM. It is assumed that the density and heat conductivity of the PCM are constant. If the temperature dependent material properties are known, the numerical methods will give more precise results for the temperature of the PCM. Thus, the material properties of the PCM should be well known in order to obtain sufficiently accurate results with the numerical methods.

Another reason for the differences between the numerical and experimental results may be in the placement of the thermocouple. The storage is filled with liquid PCM. The placement of the thermocouple may have been slightly changed. After the storage is filled up it is impossible to check the placement of the thermocouple.

It seems that natural convection is well modelled in the numerical models. The natural convection in the liquid

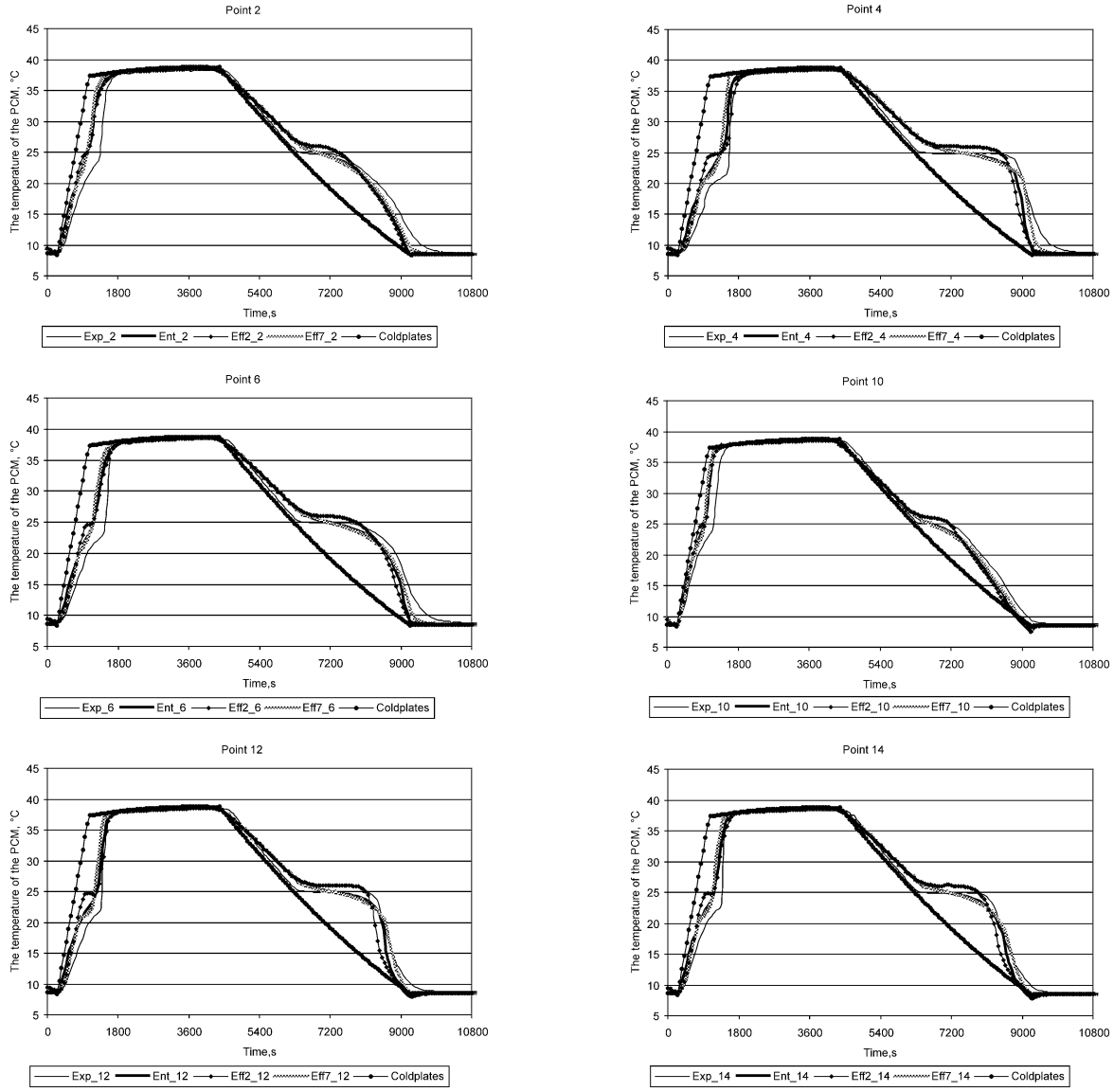

Fig. 7. The temperature of the PCM at measurement points in the PCM storage with fins, storage 2.

PCM is quite often assumed to be negligible in numerical calculations. Fig. 8 shows the experimental and numerical results of the temperature of the PCM at point 4 in the storage without the fins. The numerical results are calculated using the effective heat capacity method with a narrow phase change temperature range both with the natural convection effect and without the natural convection effect.

From the results it is possible to see that the assumption used for the natural convection coefficient gives a fairly good estimation for the behaviour of the PCM during the melting process. When the effect of natural convection is neglected in the calculation, the PCM heats up to the maximum coldplate temperature twice as slowly as it actually takes in reality. The error made is considerable and the numerical model is not performing well if natural convection is not occurring in the liquid PCM during the melting process.

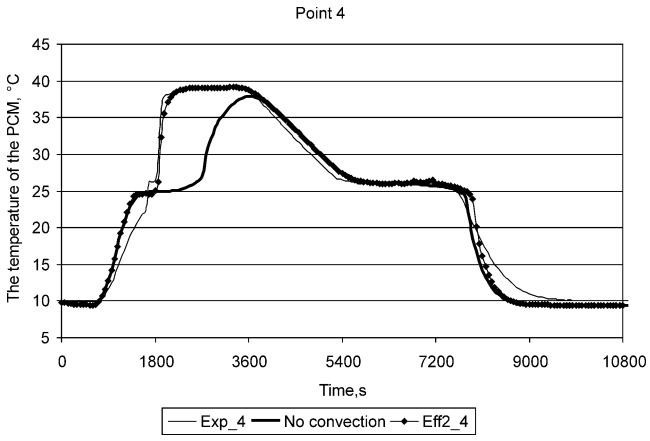

Fig. 8. The numerical results with natural convection and without natural convection and the experimental results for the temperature of the PCM.

The FEMLAB software is used in numerical calculations. It seems that FEMLAB is well suited to solving different kinds of phase change problems in one, two or three dimensions. The programme saves both time and energy. It makes it possible to change the geometry of the storage easily. For example, different kinds of heat transfer enhancement structures such as fins and honeycombs can be modelled and the effect of the structure can be seen both quickly and easily.

7. Conclusions

As can be seen from the results, both of the applied numerical algorithms seem to work reasonably well in the FEMLAB software environment. The ease that comes from being able to vary both the geometry and the parameters enables the faster design of tailored PCM storages for various electronics applications.

All the numerical predictions give a good estimation of the melting and freezing processes. However, the effective heat capacity method with a narrow temperature range, $\mathrm{d}T = 2\,^{\circ}\mathrm{C}$, is the most precise method when the results are compared to experimental results.

When the effect of natural convection is omitted in the calculation, the PCM heats up to the maximum coldplate temperature twice as slowly as it actually takes in reality. The numerical model functions poorly if natural convection is not involved in the liquid PCM during the melting process. It is essential to model natural convection in the liquid PCM during the melting process.

In the next research phase, advanced structures such as honeycombs and PCM-filled foams as well as local, separate heat sources that emulate components on a printed wiring board will be studied.

Acknowledgements

The authors would like to thank Mr. C.-M. Fager for performing the measurements, Mr. J. Manner, Mr. K. Kuittinen and Mr. M. Roos for valuable support in preparing the containers, as well as Dr. J. Rantala for providing the working environment at The Nokia Research Center. I would like to express my gratitude to Prof. K. Siren at HUT for his valuable comments during the research.

References

[1] V. Alexiades, A.D. Solomon, Mathematical Modelling of Melting and Freezing Processes, Hemisphere, Washington, DC, 1993.
[2] G.E. Myers, Analytical Methods in Conduction Heat Transfer, McGraw-Hill, New York, 1971.
[3] G. Lane, in: Solar Heat Storage: Latent Hear Material, vol. 1, CRC Press, Boca Raton, FL, 1983.
[4] J. Crank, Free and Moving Boundary Problems, Oxford University Press, Oxford, 1984.
[5] V. Voller, M. Cross, Accurate solutions of moving boundary problems using the enthalpy method, Internat. J. Heat Mass Transfer 24 (1981) 545–556.
[6] M. Costa, D. Buddhi, A. Oliva, Numerical simulation of latent heat thermal energy storage system with enhanced heat conduction, Energy Convers. Mgmt. 39 (3/4) (1998) 319–330.
[7] C. Bonacina, G. Comini, A. Fasano, M. Primicerio, Numerical solution of phase-change problems, Internat. J. Heat Mass Transfer 16 (1973) 1825–1832.
[8] Y. Rabin, E. Korin, An efficient numerical solution for the multidimensional solidification (or melting) problem using a microcomputer, Internat. J. Heat Mass Transfer 36 (3) (1993) 673–683.
[9] Comsol AB, FEMLAB Version 2.3, Reference manual, 2002.
[10] F. Incropera, D. De Witt, Fundamentals of Heat and Mass Transfer, third ed., Wiley, New York, 1990.
[11] D. Pal, Y. Joshi, Melting in a side heated enclosure by uniformly dissipating heat source, Internat. J. Heat Mass Transfer 44 (2001) 375–387.
[12] P.G. Kroeger, S. Ostrach, The solution of a two-dimensional freezing problem including convection effects in the liquid region, Internat. J. Heat Mass Transfer 17 (1973) 1191–1207.
[13] K. Peippo, Faasimuutosvaraston termodynaamiset perusmekanismit ja energiasovellutukset. (The basic thermodynamic phenomenon in phase change material storage and energy applications), Report TKK-F-B125, (1989), in finnish.
[14] R. Clarksean, Y. Chen, M. Marangiu, An analysis of heat flux limits for electronic components on a finned substrate containing a PCM, in: Advanced in Electronic Packaging 1999, vol. 2, in: EEP, vol. 26-2, ASME, 1999, pp. 1611–1616.
[15] P. Lamberg, K. Siren, Analytical model for melting in a semi-infinite PCM storage with an internal fin, Heat Mass Transfer (2002), Published in electrical version.
[16] R. Marshall, Experimental determination of heat transfer coefficient in a thermal storage containing a phase change material—The rectangular cavity, in: International Conference on Future Energy Concept, 1979, pp. 216–220.
[17] R. Marshall, Natural convection effects in rectangular enclosures containing phase change material, in: F. Kreith, R. Boehm, J. Mitchell, R. Bannerot (Eds.), Thermal heat transfer in solar energy systems, ASME, 1978, pp. 61–69.
[18] J. Eftekhar, A. Haji-Sheikh, D. Lou, Heat transfer enhancement in a paraffin wax thermal energy storage system, J. Solar Energy Engrg. 106 (1984) 299–306.
[19] K. Peippo, P. Kauranen, P. Lund, A multicomponent PCM wall optimized for passive solar heating, Energy Buildings 17 (1991) 265.
[20] The Mathworks Inc., MatLab Manual, Version 6.1, 2002.